Lagrangian Statistics in Homogeneous Isotropic Turbulence: Newtonian and Hyper-Viscous Fluids

Manuel Araújo Barjona Henriques
manuel.barjona@ist.utl.pt

Instituto Superior Técnico, Universidade de Lisboa, Lisboa, Portugal

October 2016

Abstract

An high performance computing (HPC) algorithm is developed in a Navier-Stokes solver to include the simulation of passive particles (tracers) together with hyper-viscosity. The new algorithm is shown to be highly scalable and suited to HPC simulations. Massive new direct numerical simulations (DNS) of isotropic turbulence for classical Newtonian and hyper-viscous fluids are carried out and allow the first numerical (or experimental!) verification of the theoretical results for the second order Lagrangian structure functions derived from Kolmogorov's theory, and for the Richardson law for particle pair dispersion. These results constitute a major breakthrough in the turbulence theory and will impact in engineering and geophysical simulations involving particles transport.
Keywords: Isotropic turbulence, Hyper-viscosity, High-perfomance computing, Lagrangian structure functions, Particle dispersion

1. Introduction

Almost every flow observed in nature and of engineering interest is turbulent. Turbulence strongly increases the rates of the transport and mixing of matter, momentum, and heat in a flow (in comparison with laminar flow) [1] and is crucial in engineering applications, therefore, turbulence is a subject of great interest.

There are two different perspectives to analyse a flow. The Eulerian and the Lagrangian one. The study of turbulence using a Lagrangian view was used by Taylor [2] and Richardson [3] in 1922, however, in the past seventy years the majority of research in turbulence is made considering an Eulerian view due to practical reasons since in experimental works it is easier to evaluate the velocity or a scalar quantity at fixed points. The same happens in numerical simulations where the calculations are performed in a fixed grid.

Recently a growing interest has been attracted to the Lagrangian point of view due to some facts:

1: It is a natural approach to study turbulent transport, which is of extreme importance in the development of stochastic models used for contexts as industrial mixing, cloud formation, turbulent combustion or even pollutant dispersion [4] [5] [6] [7].

2: It is now possible to experimentally perform high precision particle tracking in turbulent flows [8] [9].

3: Multi-particle statistics are an important tool to understand the evolution in time of the shape of structures within the turbulent flow and thus a better understanding of the physical mechanisms present in the energy cascade [7] [10].

Regarding aerospace engineering, the study of turbulent flows in a Lagrangian point of view is crucial for matters such as, turbulent combustion and pollutant dispersion.

The equations that describe the motion of a Newtonian fluid flow (either laminar or turbulent) are the Navier-Stokes equations. This set of equations are derived considering the conservation of mass and momentum and using the assumption that the locally stress tensor is proportional to the strain rate tensor (Newtonian fluid). Since there are only exact solutions, for this set of equations, for over-simplified cases, the study of turbulence must be made using numerical and experimental data.

To study turbulence physical mechanisms in a Lagrangian view it is desired to use Direct Numerical Simulations (DNS) to ensure that even the small scales motions are measured.

In that direction the main objectives of this work is to develop a scalable numerical code for DNS, based on pseudo-spectral schemes, with particle tracking.

Another main goal of this work is to, for the first time, quantify the effects of hyper-viscosity [11] in the Lagrangian statistics.

Finally with the results from both Newtonian

and Hyper-viscous simulations this work will address the resolution of four very important open problems: *i)* is the T3 Richardson law for particle dispersion valid? *ii)* if so, what is the universal constant in the relation? *iii)* does the second order Lagrangian structure function scales linearly? *iv)* if so, what is the universal constant in the relation?

2. Background

Unlike in the Eulerian frame, in which the statistical variable of interest is the velocity variations in space, in an Lagrangian frame, the variable of interest is the velocity variations along a particle trajectory. Thus, for the Lagrangian frame the variable of interest is:

$$\delta\vec{u}(\vec{x_0},t,\tau) = \vec{u}(\vec{x_0},t+\tau) - \vec{u}(\vec{x_0},t), \qquad (1)$$

where $\vec{x_0}$ is the initial position, t is a certain instant of time and τ an interval of elapsed time. Due to the statistically time independence (from the initial time t) and the space homogeneity (interdependency of the initial position), the Probability Density Function (PDF) of the variable will only depend on the lag time (τ). Also, due to the isotropy the PDF of each velocity component must be equal.

It is known that the n-th moment of the PDF of the velocity increments, in the inertial time range, has a universal scaling coefficient such that $\overline{(\delta u_i(\tau))^n} \sim \tau^{\xi_n}$. In the specific case of n=2, according to the Kolmogorov theory, in the inertial time range, based on the three fundamental Kolmogorov hypothesis it is possible to conclude that the scaling law regarding the 2-nd moment of the PDF of the velocity variations of a particle along time is:

$$\overline{(\delta u_i(\tau))^2} = C_2\ \bar{\epsilon}\ \tau, \qquad (2)$$

This law is believed to be universal because is linear with the dissipation rate and thus, does not required any intermittency corrections. Whether or not the scaling law is valid, has been an open problem since 1941. Note, that this law is the equivalent, in the Lagrangian frame, to the four-fifths law, and thus the answer to this question is of extreme importance both at a fundamental level, to understand if the Kolmogorov similarity theory is valid in a Lagrangian framework, and at a practical level, because knowledge of constant C_2 is crucial to the construction of stochastic models used for contexts as industrial mixing, cloud formation, turbulent combustion or even pollutant dispersion [4] [5] [6] [7].

The predicted scaling law for the Lagrangian velocity structure functions of second order (LVSF-2) have never been observed in either experiments or in numerical simulations, and it can be seen in figure 1 that, there is an absence of a plateau and the increase of Reynolds number simply leads to the increase of the peak value.

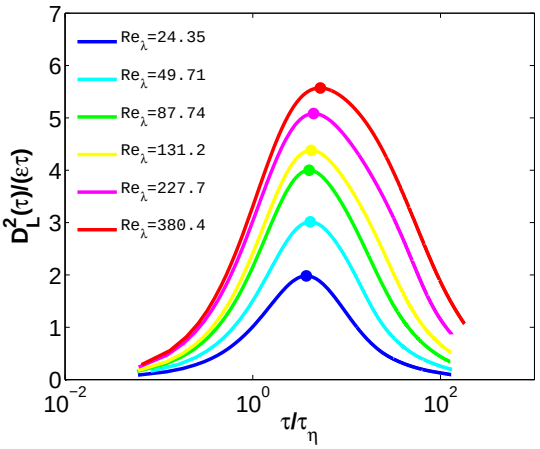

Figure 1: Lagrangian second order structure as function of Reynolds number. Six different curves are presented for Re_λ: 24; 50; 88; 131; 228; 381.

The difficulties of the observation of this scaling law are associated with small width of the inertial range which is the zone in which: $\tau_\eta \ll \tau \ll T_L$, where τ_η is the Kolmogorov micro-scale given by (where S_{ij} is the strain rate tensor):

$$\tau_\eta = (2S_{ij}S_{ij})^{-\frac{1}{2}}, \qquad (3)$$

and T_L is the Lagrangian decorrelation time given by:

$$T_L = \int_0^\infty \rho(\tau)d\tau, \qquad (4)$$

where $\rho(\tau)$ is the autocorrelation velocity function given by: $\rho(\tau) = \frac{\overline{u_i(t+\tau)u_i(t)}}{\overline{u_i(t)u_j(t)}}\frac{\delta_{ij}}{3}$.

In the Eulerian frame, the inertial range is such that $\eta \ll |\vec{r}| \ll l_0$, where η is the Kolmogorov micro-scale $\eta = (\frac{\nu^3}{\epsilon})^{\frac{1}{4}}$ and l_0 is the characteristic length scale regarding the largest eddies. Unlike the Lagrangian statistics, the scaling laws regarding the inertial zone in a Eulerian frame of work, such as the four-fifths law [12], are observed for small Reynolds number (Re_λ). This situation is believed to result from the fact that $\frac{T_L}{\tau_\eta} \sim Re_\lambda$, while, $\frac{l_0}{\eta} \sim Re_\lambda^{\frac{3}{2}}$, and thereby, the same increase of the Reynolds number cause an higher extension of the inertial range in the Eulerian frame than in the Lagrangian frame. In such way that has been predicted that a clear plateau will only be observed for Reynolds numbers higher than 30000, while until now the highest Reynolds achieved was ≈ 1000 [13] [14].

Since the evaluation of scaling coefficients regarding the PDF moments of the Eulerian veloc-

ity structure function has been extensively studied [15], it is tempting to connect the Eulerian and Lagrangian statistics. In that direction, multifractal theory [16] has been applied in an attemp to try to connect the Eulerian and Lagrangian fractal dimension [17] [18] [19] [20]. All the models developed with the multifractal formalism, with more or less accuracy, predict that $\xi_2 = 1$, therefore, also in order to check whether the multifractal formalism correctly connects Eulerian and Lagrangian frames it is important to observe experimentally the scaling law given by equation (2).

Regarding the Lagrangian velocity structure function of order n (LVSF-n), for $n \neq 2$, it is also of extreme importance to evaluate the scaling coefficients (ξ_n). However, if the inertial range width for the experimental data is not sufficient to observe a scaling law for LVSF-2, it definitely will not be sufficient to capture scaling laws for moments of higher order. To attempt computing the coefficients ξ_n, in a similar way as the procedure used in the Eulerian frame, one can use the extended self-similarity, according to which the following relation holds: $\overline{(\delta u_i^+(\tau))^n} = A_n \overline{(\delta u_i^+(\tau))^m}^{\frac{\xi_n}{\xi_m}}$. Therefore, the slope in a log-log plot of $\overline{(\delta u_i^+(\tau))^n}$ as function of $\overline{(\delta u_i^+(\tau))^m}$ is $\frac{\xi_n}{\xi_m}$. Using this approach, in order to compute the coefficient ξ_n, one must know the coefficient ξ_m. This is another reason why the verification of the scaling law (2) is absolutely crucial, because it can also be used as the comparison coefficient. Presently the computation of ξ_n is made using $\xi_2 = 1$ (m=2), however as explained no experimental evidence of this law has yet been found thus, the existing predictions of ξ_n, using this method, can be completely wrong.

Particles can be trapped in a vortex filament, thereby, the tracers are an important tool to study the physical mechanism in these structures, this is one of the major advantages of the Lagrangian approach. When a particle is trapped in one of these structures, it experiences high velocity fluctuations, therefore, this extreme events must have some influence in the LVSF-n functions. In order to analyse these effects, first there must be applied a criteria to differentiate whether or not a particle experiences these effects. In [21] it was used as criteria that a particle experienced a trapping event if the mean absolute value of the acceleration, during a time lag $2\tau_\eta$, was at least seven times superior than the root mean square of the acceleration of all particles. Filtering the statistics in order to exclude the particles that were trapped, it was possible to conclude that, the saturation of the scaling exponents ξ_n over the constant 2, for $\tau_\eta < \tau < 10\tau_\eta$ is the signature of this trapping events. By saturation of the coefficient is meant that $\lim_{n\to\infty} \xi_n = 2$, also, it is important to outline that the duration of these extreme events is also in the interval $[\tau_\eta; 10\tau_\eta]$.

Another statistical variable of interest is a particle displacement between its position and the center of mass of a cluster of particles (in which the particle is embodied) in a turbulent flow. The study of this subject, the turbulent relative dispersion, has innumerable applications. Cloud formation is one of the most interesting ones [3] [22]. Also, it is possible to relate the Lagrangian statistics of particle dispersion with the statistics of passive scalars, therefore, particle dispersion is important in the study of turbulent mixing, combustion and pollution [23].

This variable can be defined as:

$$\delta\vec{r}^+(t,\tau) = \vec{r}^+(t+\tau) - \vec{r}^+(t), \tag{5}$$

where $\vec{r}^+(t)$ is the distance between the particle position and the center of mass (this distance, for the initial time, is also denoted by $\vec{r}_0^+$). Once more, the statistics are independent of the initial time (they do not depend on t), and due to isotropy, the statistics of this variable are independent of the direction therefore, the variable of interest is simply:

$$\delta|\vec{r}^+(\tau)| = |\vec{r}^+(t+\tau)| - |\vec{r}^+(t)|. \tag{6}$$

In 1926, L.F. Richardson, using experimental results, obtained by releasing balloons and measuring the position where they land and the time travelled, notice that the root mean square of the variable (6) was proportional to the cubic power of time [22]. However, only in 1950, using the Kolmogorov similarity theory, G. Batchelor, stated that in the inertial time sub-range the variance, for initial separation in the inertial subrange, is given by [24]:

$$\overline{(\delta|\vec{r}^+(\tau)|)^2} = g\epsilon t^3, \tag{7}$$

where g is a universal constant. This law is known as the T3 Richardson law, which is assumed to be universal. However, this relation has never been experimentally observed, and like the scaling law of the LVSF-2 it is assumed that the reason why this scaling law has not yet been been seen is due to the limitations of the Reynolds number. Some estimations were made for the constant g which is supposed to be $g \approx 0.6$, however, only for a very small range of initial separations it is possible to observe, poorly, the scaling law [25]. Thus, whether or not the scaling law (7) is valid is a fundamental problem in turbulence.

2.1. Homogeneous Isotropic Turbulence

The specific case that will be studied in this thesis work is the Homogeneous Isotropic Turbulence (HIT). The principal characteristic of HIT is that the statistics regarding the random motions of the

fluid are independent of the position. This flow is idealized and rigorously it does not exist in nature because there is always some space dependence of the statistics. This dependence can be reduced using grid generated turbulence, which is the type of turbulence more close to the idealized HIT, and the one used in experimental investigation [26].

The reason to study HIT is because it is the simplest type of turbulence and since the scaling laws and physical mechanisms of turbulence are universal, then, they can be studied in this idealized flow. An example of 200 particles trajectories in an HIT simulation is shown in figure 2.1.

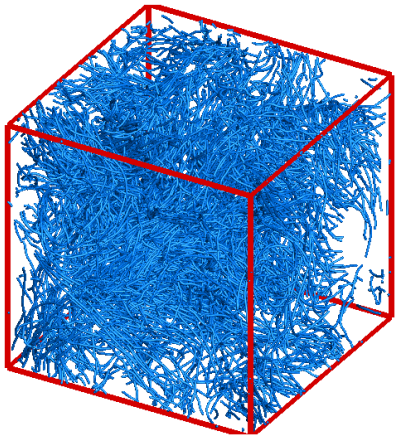

Figure 2: Trajectories of 200 particles in an HIT simulation carried out in this work.

2.2. Hyper-viscosity

The inertial range is characterized by energy transfer flux from larger scales to smaller scales, where it is dissipated. The intermediate scales, where the energy is transfered only by means of inertial forces is called inertial-range region. The understanding of the physical mechanisms in this range is of extreme importance because it is believed that the scaling laws, regarding this region, are universal. Therefore, it is natural to suppose that the way energy is extracted from the the flow does not influence the properties of the inertial range [11].

In an attempt to test if the previous supposition is valid, Vadim Borue, replaced the normal Laplacian component of the Navier-Stokes equations by a higher power of the Laplacian. The Laplacian term, in a mathematical point of view, is the one responsible for the dissipation of energy in the flow, thus, a flow in which the dissipation is proportional to a higher order power of Laplacian is denominated as hyper-viscous flow [11].

Using Hyper-viscosity in DNS as been proven to have no affect in the inertial range scaling laws while it effectively increases, by an order of magnitude, the extent of the inertial range and thus the equivalent Reynolds number of the flow [27] [11] [28] [29].

The major problem in the study of the Lagrangian statistics is that the Reynolds number achievable using DNS of Newtonian fluids is not high enough to observe an inertial scaling zone. Therefore, one may wonder, whether the use of Hyper-viscosity will affect the Lagrangian statistics. This is one of the fundamental question that this thesis pretends to answer.

The Hyper viscosity modified Navier-Stokes momentum equations are [11]:

$$\frac{\partial u_i}{\partial t} + u_j \frac{\partial u_i}{\partial x_j} = -\frac{1}{\rho}\frac{\partial p}{\partial x_i} + (-1)^{h+1}\nu_h \nabla^h u_i + f_i, \quad (8)$$

in which, h is the hyper viscosity coefficient. In all simulations performed here h was taken to be $h = 8$. Also, ν_h is the hyper-viscosity coefficient that is chosen to be such that [11]

$$\nu_h (\frac{N}{2})^{2h} \Delta t = 0.5 \ . \quad (9)$$

To compute the equivalent Reynolds, the following formula will be used [11]:

$$Re_\lambda = C_h (\frac{k_d}{k_f})^{\frac{2}{3}}. \quad (10)$$

Where k_d is the wavenumber where the maximum of vorticity occurs (in the spectrum) and k_f is where the forcing peak is localized. Finally C_h is a contant that depends on the hyper-viscosity coefficient. For $h = 8$, $C_8 \approx 50$.

3. Implementation

The code implemented solves directly the Navier-Stokes equations for an HIT simulation. The domain used is a box with dimension $(2\pi)^3$ with periodic boundary conditions. The code uses, as spatial discretization, spectral schemes where de-aliasing is made applying a spectral cut-off filter [30], where the cut-off wavenumber is $k_{cut} = \frac{2}{3}k_{max}$ (where k_{max} is the maximum wave-number that guarantees the verification of the Nyquist-Shannon sample theorem). The temporal discretization is an explicit third order low storage Runge-Kutta scheme [31], the time step used in each iteration is such that the Courant number $C_{fl} = \frac{\Delta t}{\Delta x}|u|_{max}$ condition used is $C_{fl} \leq 0.6$, except for hyper-viscosity simulations in which the stability condition is more restrictive and the Courant number must be such that $C_{fl} \leq 0.2$. To ensure that a statistical stationary state is achieved it is required to inject energy, the forcing method used in the code is described in [32]. The particle velocity interpolation is made using a cubic Lagrangian polynomial.

To handle parallel computation the code implemented uses *2DECOMP&FFT* library [33]. It is a

software framework designed for large-scale parallel applications using three-dimensional structured mesh. Using this library, the whole domain is decomposed in 2D pencils as shown in figure 3, and each processor deals with the data regarding its sub-domain. To deal with communications between cores, it relies on Message Passing Interface (MPI).

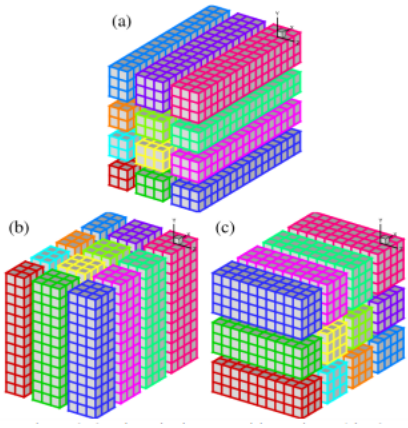

Figure 3: 2D domain decomposition using a 4 by 3 processor grid. Source: [33].

A very important feature is that it also provides a highly scalable and efficient interface to perform three-dimensional FFTs. The one that will be used here is the Fast Fourier in the West (FFTW) [34]. By using this software it is possible to obtain scalability for a number of cores until the order of $\sim 10^5$.

3.1. Code Development

The numerical work developed and implemented in this work concerns the particle tracking and hyper-viscosity. To obtain a scalable code, the synchronous communications must be avoided, however since particles roam across the entire domain the processors must communicate between each other thus, fully parallelization of the code can be difficult to achieve. The key aspects of the code that ensure the scalability will be detailed next.

3.1.1 Particle transfer

As stated previously, the domain is decomposed into sub-domains and each core processor handles the computations regarding its specific 2D pencil. However, particles move freely in the box and thus, in any sub-step a particle can exit a processor domain to enter into another one. However, the communications are very expensive and should be avoided to ensure the scalability of the code.

Therefore, in the present work, the particle transfers between processors are only made at the end of each time step, thus the communication time is reduced by a third. Even though particles change domain (i.e. processor and 2D-pencil) during a sub-step, there is no need to do particle data transfers among processors in each sub-step, the way this property is achieved will be detailed in section 3.1.2.

Also, in a synchronous communication the processors will stop until all of them are ready for the data transfer. Therefore, sending particles one by one is computationally extremely expensive so, the particle transfer routine must have the lowest communication requests as possible. Keeping this in mind, the solution found in the present work consists in creating an auxiliary matrix (M_{aux}) with dimensions 5xT_N and fill it with info of the particles that must be transferred. The number of columns of the matrix , T_N, is such that will be always grater than the number of all transfers between domains in a time-step (to prevent data leakage). The number of lines is 5 so that each column has the information about the particle coordinates (3), the particle ID (1) (a variable that greatly simplifies the post-processing tools making it possible to reconstruct the particle trajectory and properties variations along each one) and the ID of the processor that contains the domain/2D-pencil in which the particle currently is (1). The processor that emanate the particle, computes the ID of the processor in which the tracer should be, if it is equal to his own ID, there is no need for transfer otherwise there is. Since the new processor ID has already been computed it saves computational time sending this information instead of making all processors recompute it to know whether or not the particle is in its domain. The additional memory cost of this approach is, using an overestimation, over 10 MegaBytes consequently, in a processor with 4 GibaBytes of memory RAM the increase in RAM is negligible.

Before filling matrix M_{aux} and make the particle transfer all processors must compute how many particles exited its domain. After that, all of them fill an auxiliary array, A_{aux} (that has a dimension equal to the number of processors), with zeros except at the entry number equal to their own processor ID, in which they stored the number of particles exiting their domain.

Then, the first synchronous communication is made to assemble all A_{aux} of all processors into a new B_{aux} array . Notice that B_{aux} is an array that for each entry have the number of particles exiting the processor with the ID equal to the entry number. If T_N is smaller than the sum of all entries of the array (total number of transfers), it must be updated, but, this rarely occurred in the present simulations.

After knowing B_{aux} it is possible to fill the matrix M_{aux}. To do so, each processor sums the number of particles that have exited the processors with an

ID number lower than its own and fills that number of columns with zeros. After that it fills the next columns with the info of the particles that are exiting his domain. The remaining columns are also set to zero.

Following this step, a second synchronous communication is made to sum all M_{aux} of all processors. Notice that the final result (N_{aux}) is a matrix with all the particles that are changing domain. After that, each processor scroll along the fifth line of N_{aux} and whenever the value found is equal to his own ID, it stores the particle. Notice that the choice of the matrix dimensions as 5xN_T instead of N_Tx5 was not random, actually it was made concerning this step because it is more efficient to scroll in a matrix line than in a matrix column.

Finally, for writing the particle states it is also necessary that all processors know how many particles are in each processor. The way to do this is similar to the one described previously regarding the exit number particles. Meaning that another synchronous communication is added.

In conclusion, the method implemented has only 3 synchronous communications and an unimportant setback due to a small increment in memory usage. It is relevant to state that this routine was of crucial importance to ensure the scalability of the code.

3.1.2 Particle Velocity Interpolation

The cubic interpolation requires the usage of 4 cell nodes in each direction (x,y and z), however, suppose that a particle is so close to the boundary of two domains that in order to complete the interpolation, it is required to use the velocity field from points that are out of the processor domain. This situation could be resolve by an information trading between two, or three or even four processors. However, as already explained, the number of communications must be the smallest possible, therefore the solution to this, rests in the use of Halo cells, i.e., each processors during the interpolation also has the information of its neighbour points. The halo can have different levels, the level one case, for a 2D domain decomposition using a 2x2 MPI processes, is illustrated in figure 4.

The 2DECOMP library has halo-cell support routines which are easy and efficient, and that have been used for this purpose.

Finally it is important to state that, due to the stability conditions (regarding the Courant number) a particle can never cross an entire cell. Knowing that the halo level can be chosen in such way that even if during a sub-step a particle change processor domain the interpolation will still be feasible. As a result, it is possible to transfer particles only in the end of time step instead of in every sub-step and consequently reduced the synchronous communication by a third.

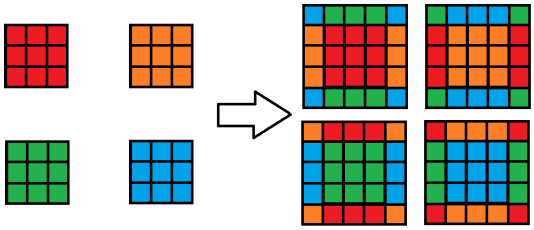

Figure 4: Illustration of level 1 halo cells for a 2D domain decomposition using a 2x2 MPI processes.

3.1.3 Particle states writing and Post-Processing

The particle states writing, in order to be time efficient, is made by blocks, i.e., each processor has an exclusive portion of the output file and writes the states of its particles. For this purpose, as discussed in section 3.1.1 every processor knows the number of particles that are in each processor (this is the reason why the third and last synchronous communication, in the particle transfer routine, is made). With that input, for a given number of particle fields to be stored (e.g. x, y, z, u, v, w), it is possible to compute the number of bytes that each processor will occupy in the file (number of particles times the number of bytes needed to store the number of given fields). To compute the specific location where a processor will start writing it is only required to sum the number of bytes that each processor has, with an ID number lower than its own.

Notice that the particles are not written always in the same sequence. This is why it is so important to have an extra field with the particle ID. Only that field enables the reproduction of the particle trajectories and analysis of property variations along each single particle, during the Post-Processing execution.

Finally, another important feature is that during the Post-Processing, every time-step is considered as the launch of another simulation. It is obvious that each new simulation will have a running time smaller than the previous one. However, the number of samples used to compute statistics regarding property variations in a time interval, pertaining the inertial range of time, will be the number of particles multiplied by a factor of the order of $\sim 10^4$ *i.e.* the time step. Therefore the number of particles required to have a converged statistical results is tremendously reduced. These reduction also results in a critical reduction of computational time spent and in a massively decrease in memory usage.

4. Results

4.1. Scalability Verification

One of the main objectives of the present thesis was to develop a scalable code, i.e., a code in which the computational time per time-step must be inversely proportional to the number of processors used. To verify if this property was achieved scaling tests were performed in 4 supercomputers. Here it will be just shown the results for the supercomputer 'HAZELHEN'. The processor of this supercomputer are Intel Xeon CPU E5-2680 v3, with 128 GB of memory Ram per node, with 24 cores per node, a peak perfomance at 7.42 Pflops and with Cray Aries intercommunication technology. The other supercomputers give similar results, but are not shown here due to lack of space.

For any graphical representation regarding the iteration time as function of number of processors, two different zones are expected to be observed. The first one, regarding a low number of processors, in which the time spent in communications is much smaller than the time spent on actual computation and thus, an increase of number of processors is followed by a decrease in the inverse proportion of the time spent per iteration (zone where scalability is observed). The second one, regarding a high number of processors, in which the communication time is similar, or higher, than the time spent on actual computations and an increase in the number of processors does not lead to a decrease in inverse proportion of the time spent per iteration and it can even increase the computational time. This is the reason why, as stated in section 3.1, the communications must be avoided by all means to ensure a more wide scalable zone.

Before presenting the results obtained it is important to state that starting point of this work was a DNS code and the implementations made in the present work only added two new functionalities: the possibility of particle tracking and the possibility of simulating a flow with Hyper-viscosity. From the pre-existing version of the code, it was observed that it was scalable approximately until the number of processors was near the number of grid points in each direction. Thereby, since the scalability zone will certainly not be increased with the two new functionalities, the main objective is to keep it unaltered.

The scaling curves obtained from the simulations performed in 'HAZELHEN' are shown in figure 5.

Analysing figure 5 it is possible to see that the region where the code is scalable was unaltered, i.e., the code is scalable until the number of processors is similar to the number of grid points in each direction. Thus, the implementation of the particle tracking was excellent!

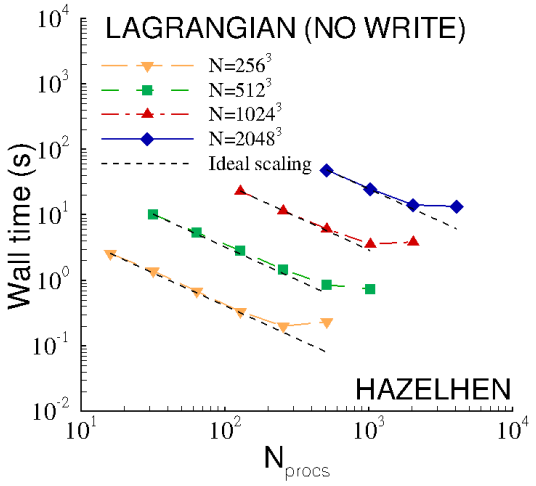

Figure 5: Hazelhen computational time of an iteration, without writing, as function of number of processors.

4.2. Hyper-viscosity effect on Lagrangian statistics.

The main advantage of using Hyper-viscosity is that it allows to simulate turbulent flows with higher Reynolds numbers than a simulation, for the same number of grid points, with a Newtonian fluid. Since the Lagrangian inertial range has never been observed due to the limited Reynolds number achievable in Newtonian fluid simulations, one hypothesis arises: 'can Hyper-viscosity be used to compute the LVSF-2 in the inertial range?' .

Using Hyper-viscosity it is possible to observe that the principle characteristics of Lagrangian statistics are unaffected. This characteristics are for example the, shape evolution of the PDF from exponential tail to Gaussian and the exponential decay of the correlation function. However, to confirm the hypothesis, one should compare the inertial scaling zones for both Newtonian and Hyper-viscous fluids, however, since this zone has not yet been observed, it will be compared the evolution of the LVSF-2 with the Reynolds number for both fluid models.

The evolution of the LVSF-2 for the three simulations with the lowest Reynolds is shown in figure 6. Comparing with figure 1 it is possible to see that in both cases, the increase of Reynolds had cause the increase of the peak value (C_0^*), and also an increase of the lag time where the peak occurs (τ_0^*). Thus, for both Newtonian and Hyper-viscous fluids the increase of Reynolds causes qualitatively the same effects in the LVSF-2.

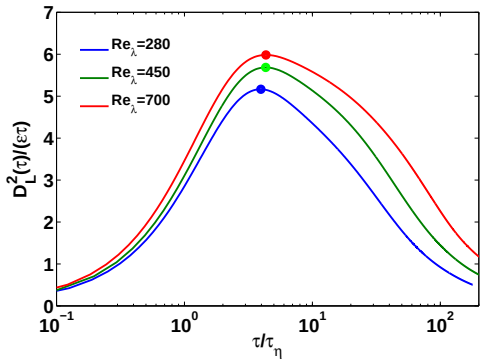

Figure 6: LVSF-2 as function of Reynolds number for simulation with with Hyper-viscosity.

To analyse if Reynolds number increase effect has a similar quantitative effect in Hyper-viscous simulations, one evaluates the increase in the peak value (C_0^*) as function of Re_λ in both fluids. As stated before, due to anisotropic fluctuations, there is an uncertainty in the LVSF-2. Since the three components have different peak values ($C_0^i = max(\frac{\overline{(\delta u_i^+(\tau))^2}}{\epsilon\tau})$), the uncertainty of C_0^* is computed as the $max(|C_0^* - C_0^i|)$, with $i \in \{1, 2, 3\}$. The results of C_0* as function of Re_λ are shown in figure 7, in this figure is also plotted a fitting curve, given by $C_0^* = 6.5(1 + \frac{70}{Re_\lambda})^{-1}$, that B. Sawford obtained from his results [25] (the curve is not exact and it is used to compare the trend).

Analysing figure 7 one concludes that Hyper-viscosity accurately predicts the evolution of C_0^* as function of Reynolds number.

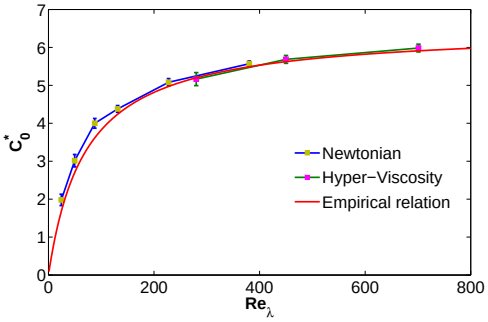

Figure 7: Evolution of the peak value C_0^* as function of Reynolds for both Newtonian and Hyper-viscous fluids. An empirical relation obtain in [25] is also plotted for comparison purposes.

Finally a comparison between Hyper-viscous and Newtonian fluids will be made for the scaling coefficient ζ_4. To compute this coefficient it was used an Hyper-viscous simulation with $N = 1024$. Even though there is an absence of the inertia range, for low Reynolds numbers it is possible to compute the inertial scaling coefficients using self-similarity [35]. The evolution of ζ_4 with time is shown in figure 8.

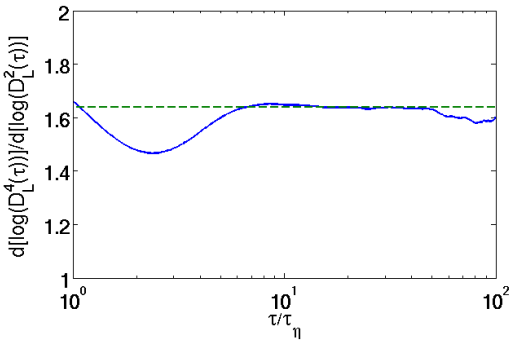

Figure 8: Scaling coefficient of the LVSF-4, obtained from an Hyper-viscous simulation with $Re_\lambda = 1102$. The green dashed line has the constant value of 1.64.

From this figure, three relevant facts must be highlighted:

Second, the green dashed line has a constant value of $\zeta_4 = 1.64$. This value was computed by averaging the plotted function in the interval $[10\tau_\eta; 40\tau_\eta]$. To estimate the uncertainty of the scaling coefficient it is used the maximum difference between ζ_4 computed with the mean value of the three velocity components and ζ_4^i computed using only the i-th component.

Thus, using Hyper-viscosity, it is obtained that the scaling coefficient of the LVSF-4, in the inertial range, is $\zeta_4 = 1.64 \pm 0.03$. In [19] the value estimated for this constant was $\zeta_4 = 1.66 \pm 0.02$, thus, the result obtained using Hyper-viscosity is consistent with the one obtained in DNS simulations using Newtonian fluid. Therefore, this is a clear proof that the Hyper-viscosity can be used to obtain the scaling coefficients in the inertial zone.

4.3. LVSF-2 dependence with Reynolds number

We have seen in the previous section that Hyper-viscosity can be used to study the LVSF-2. Until now, the largest Reynolds for which the Lagrangian statistics had been studied was approximately 1000, however, in the presented work two simulations with higher Reynolds number were carried out, one with $Re_\lambda = 1102$ and other with $Re_\lambda = 1774$, therefore, we are able to study this function like it never had been studied, and in a position that had never been achieved by no one else. Our principal concern is to try verify if $\zeta_2 = 1$, an open problem since 1941.

In order to prove the theory, two things must be observed: 1- The function $D_L^2(\tau)$ when adimensionalyzed by $\epsilon\tau$, must show a clear plateau, i.e., a zone where the function is constant in the value C_0, an

universal constant. 2- In the K41 theory, it is assumed isotropy is the small scale, thus, the law is only valid if C_0 a is equal for the three components. The LVSF-2 obtained for different Reynolds numbers is shown in figure 9.

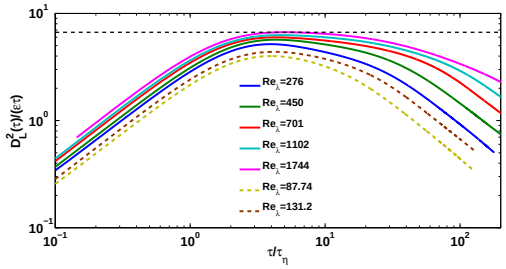

Figure 9: LVSF-2 for different Reynolds numbers. Solid lines are curves obtained with Newtonian simulations while dashed lines are curves obtained using Hyper-viscosity simulations.

To conclude whether or not, in figure 9 for the highest Reynolds number, there is already a plateau, it will be evaluated the width of the interval were $\frac{D_L^2(\tau)}{\epsilon\tau} > 0.99C_0^*$. The interval were this condition is valid is approximately: $[3.8\tau_\eta; 7.2\tau_\eta]$, thus, the width of this interval, in a log-log plot, is 28% of a decade. Also, the inertial range must be such that $\tau_\eta \ll \tau \ll T_L$, the width of the interval $[\tau_\eta; 77]$ is 188% of a decade, therefore, a plateau is observed in about 15% of the overestimated width of the inertial range.

To evaluate if the second requirement is fulfilled it will be used analysed the value of the parameter $e = \frac{max(|C_0^* - C_0^i|)}{C_0^*}$. This value, for the simulation with the largest Reynolds is $e = 0.002$, which is the smallest value for all simulations, thus small relative differences exist between the three components and so, one concludes that indeed the isotropy exists and so the second requirement is fulfilled.

To conclude, it had been presented clear evidences, for the first time in 75 years of investigation, that corroborate the existence a linear scaling law for the LVSF-2. The predicted value for the universal constant is $C_0 = 6.7$.

4.4. Dispersion statistics dependence with Reynolds number

In turbulence since the analysis is statistic, one must evaluate all the moments of any order of the PDF of $\delta|\vec{r}^+(t,\tau)|$. The moment of n-th order is given by:

$$\overline{(\delta|\vec{r}^+(t,\tau)| - \overline{\delta|\vec{r}^+(t,\tau)|})^n}. \qquad (11)$$

However, is assumed that, as consequence of the mean velocity in HIT is 0, then $\overline{\delta|\vec{r}^+(t,\tau)|} = 0$. However this is not a valid approximation and therefore, in this work the second order moment will be analysed without it. Since, as seen before, Hyper-viscosity can be used to compute Lagrangian statistics, then, it will also be used here to obtain curves for higher Reynolds numbers. The curves obtained are plotted in figure 10, and it is clear there is the tendency to a plateau as the Reynolds number increases. Also, for the simulation with $Re_\lambda = 1744$ that plateau already exist as can be seen in figure 11. This is the first time that a clear plateau was observed from direct measurements. Also, even though all the curves in figure 11 do not yet show a plateau, analysing figure 10 it is clear that, as the Reynolds increases, all the curves are converging. The expected is that they all converge to the constant line with value 0.165.

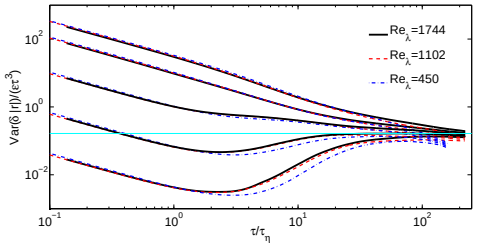

Figure 10: Relative dispersion plots dependence with Reynolds number, for initial separations of, from bottom to top, $\frac{r_0^+}{\eta}$: 0.25; 1; 4; 16; 64. This results are for Hyper-viscous fluids. The cyan line has the constant value of 0.165.

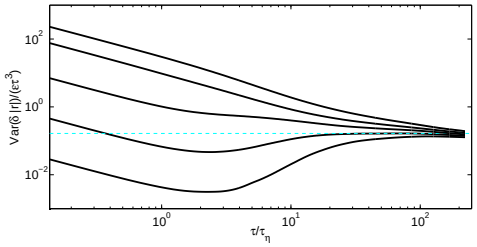

Figure 11: Relative dispersion plots dependence with Reynolds number, for initial separations of, from bottom to top, $\frac{r_0^+}{\eta}$: 0.25; 1; 4; 16; 64. This results the simulation carried out in this work the highest Reynolds. The cyan line has the constant value of 0.165.

Also, the motivation to realize this statistics was that the mean distance between two particles is not constant. In figure 12 the mean value is plotted and it is visible that the hypothesis is only valid for small time lags, also in that figure 12 there are two cyan lines that define the limits of the inertial length range, the lowest one is the dimension of the dissipative scales η and the other one the dimen-

sion of the largest eddies l_0. Comparing figures 11 and 12 it is possible to observe that the region were the scaling law is observed is exactly in the inertial length range!

Considering all this, we believe that, after 90 years of discussion, it has been finally proved that the T3 law is valid. Also the universal constant expected is $g = 0.165$.

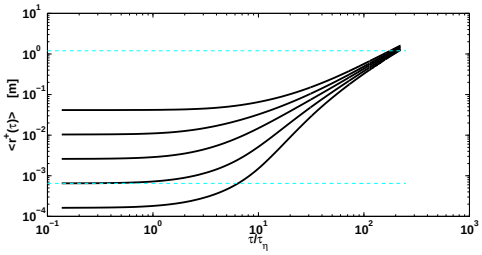

Figure 12: Mean distance between particles as function of time, from bottom to top, $\frac{r_0^+}{\eta}$: 0.25; 1; 4; 16; 64. This results the simulation carried out in this work the highest Reynolds. Cyan lines define the limit values of the inertial scale length range.

5. Conclusions

An high perfomance computing (HPC) algorithm was developed in a Navier-Stokes solver for including the simulation of passive particles (tracers) together with hyper-viscosity. The new algorithm is shown to be highly scalable and suited to HPC simulations. Massive new direct numerical simulations (DNS) of isotropic turbulence for classical Newtonian and hyper-viscous fluids are carried out and allow the first numerical (or experimental!) verification of the theoretical results for the second order Lagrangian structure functions derived from Kolmogorov's theory, and for the Richardson law for particle pair dispersion. These results constitute a major breakthrough in the turbulence theory and will impact in engineering and geophysical simulations involving particles transport.

References

[1] A. S. Monin and A. M. Yaglom. *Statistical fluid mechanics: mechanics of turbulence, Vol. 1*. M.I.T. Press, Cambridge., 1975.

[2] G. I. Taylor. Diffusion by continuous movements. *Proc. London Math Soc.*, pages 196–212, 1922.

[3] Lewis Fry Richardson. *Weather prediction by numerical process*. Cambridge University Press, 1922.

[4] S. B. Pope. *Turbulent Flows*. Cambridge University Press, 2000.

[5] S B Pope. Lagrangian pdf methods for turbulent flows. *Annual Review of Fluid Mechanics*, 26(1):23–63, 1994.

[6] P. K. Yeung. Lagrangian investigations of turbulence. *Annual Review of Fluid Mechanics*, 34(1):115–142, 2002.

[7] Katepalli R. Sreenivasan Peter A. Davidson, Yukio Kaneda. *Ten Chapters of Turbulence*. Cambridge University Press, 2013.

[8] N. Mordant, P. Metz, O. Michel, and J.-F. Pinton. Measurement of Lagrangian velocity in fully developed turbulence. *Physical Review Letters*, 87:214501, Nov 2001.

[9] R. Volk, N. Mordant, G. Verhille, and J.-F. Pinton. Laser doppler measurement of inertial particle and bubble accelerations in turbulence. *EPL (Europhysics Letters)*, 81(3):34002, 2008.

[10] A. Pumir, B. I. Shraiman, and M. Chertkov. The lagrangian view of energy transfer in turbulent flow. *EPL (Europhysics Letters)*, 56(3):379, 2001.

[11] V. Borue and S. A. Orszag. Forced three-dimensional homogeneous turbulence with hyperviscosity. *EPL (Europhysics Letters)*, 29(9):687, 1995.

[12] A. N. Kolmogorov. On degeneration of isotropic turbulence in an incompressible viscous liquid. *Dokl. Akad. Nauk. SSSR*, 31:538–541, 1941.

[13] Brian L Sawford and PK Yeung. Kolmogorov similarity scaling for one-particle Lagrangian statistics. *Physics of Fluids (1994-present)*, 23(9):091704, 2011.

[14] L Biferale and AS Lanotte. About the second order moment of the Lagrangian velocity increments. *University of California Santa Barbara, Kavli Institute Preprint, NSF–ITP–11–103*, 2011.

[15] U. Frisch. *Turbulence*. Cambridge University Press, 1995.

[16] U Frisch and G Parisi. Fully developed turbulence and intermittency. *Turbulence and predictability in geophysical fluid dynamics and climate dynamics*, 88:71–88, 1985.

[17] MS Borgas. The multifractal Lagrangian nature of turbulence. *Philosophical Transactions of the Royal Society of London A: Mathematical, Physical and Engineering Sciences*, 342(1665):379–411, 1993.

[18] G Boffetta, F De Lillo, and S Musacchio. Lagrangian statistics and temporal intermittency in a shell model of turbulence. *Physical Review E*, 66(6):066307, 2002.

[19] R Benzi, L Biferale, R Fisher, DQ Lamb, and F Toschi. Inertial range Eulerian and Lagrangian statistics from numerical simulations of isotropic turbulence. *Journal of Fluid Mechanics*, 653:221–244, 2010.

[20] Laurent Chevillard and Charles Meneveau. Lagrangian dynamics and statistical geometric structure of turbulence. *Physical review letters*, 97(17):174501, 2006.

[21] Luca Biferale, Guido Boffetta, Antonio Celani, Alessandra Lanotte, and Federico Toschi. Particle trapping in three-dimensional fully developed turbulence. *Physics of Fluids (1994-present)*, 17(2):021701, 2005.

[22] Lewis F Richardson. Atmospheric diffusion shown on a distance-neighbour graph. *Proceedings of the Royal Society of London. Series A, Containing Papers of a Mathematical and Physical Character*, 110(756):709–737, 1926.

[23] Brian Sawford. Turbulent relative dispersion. *Annual review of fluid mechanics*, 33(1):289–317, 2001.

[24] GK Batchelor. The application of the similarity theory of turbulence to atmospheric diffusion. *Quarterly Journal of the Royal Meteorological Society*, 76(328):133–146, 1950.

[25] Brian Lewis Sawford, Pui-Kuen K Yeung, and Jason F Hackl. Reynolds number dependence of relative dispersion statistics in isotropic turbulence. *Physics of Fluids*, 20(6):065111–1 – 065111–13, 2008.

[26] G. K. Batchelor. *The Theory of Homogeneous Turbulence*. Cambridge University Press, 1953.

[27] Vadim Borue and Steven A. Orszag. Numerical study of three-dimensional kolmogorov flow at high reynolds numbers. 306:293–323, 2006.

[28] Kyle Spyksma, Moriah Magcalas, and Natalie Campbell. Quantifying effects of hyperviscosity on isotropic turbulence. *Physics of Fluids*, 24(12), 2012.

[29] A. G. Lamorgese, D. A. Caughey, and S. B. Pope. Direct numerical simulation of homogeneous turbulence with hyperviscosity. *Physics of Fluids*, 17(1), 2005.

[30] Claudio Canuto, M Yousuff Hussaini, Alfio Maria Quarteroni, A Thomas Jr, et al. *Spectral methods in fluid dynamics*. Springer Science & Business Media, 2012.

[31] J. H. Williamson. Low-storage Runge-Kutta schemes. 35:48–56, 1980.

[32] K. Alvelius. Random forcing of three-dimensional homogeneous turbulence. *Physics of Fluids*, 11(7):1880–1889, 1999.

[33] N. Li and S. Laizet. 2decomp&fft - a highly scalable 2D decomposition library and fft interface. In *Cray User Group 2010 Proceedings*, Edinburgh, 2010.

[34] Matteo Frigo and Steven G. Johnson. The design and implementation of FFTW3. *Proceedings of the IEEE*, 93(2):216–231, 2005.

[35] R Benzi, S Ciliberto, R Tripiccione, C Baudet, F Massaioli, and S Succi. Extended self-similarity in turbulent flows. *Physical review E*, 48(1):R29, 1993.